AIAA 93-0814

Deformation and Secondary Breakup of Drops

L.-P. Hsiang and G. M. Faeth
Department of Aerospace Engineering
The University of Michigan
Ann Arbor, MI

31st Aerospace Sciences Meeting & Exhibit
January 11-14, 1993 / Reno, NV

DEFORMATION AND SECONDARY BREAKUP OF DROPS

L.-P. Hsiang* and G. M. Faeth†
Department of Aerospace Engineering
The University of Michigan
Ann Arbor, MI 48109-2140, U.S.A.

Abstract

Drop properties during and after secondary breakup in the bag, multimode and shear breakup regimes were observed for shock wave initiated disturbances in air at normal temperature and pressure. Test liquids included water, n-heptane, ethyl alcohol and glycerol mixtures to yield Weber numbers of 15-600, Ohnesorge numbers of 0.0025-0.039, liquid/gas density ratios of 579-985 and Reynolds numbers of 1060-15080. Measurements included pulsed shadowgraphy and double-pulsed holography to find drop sizes and velocities after breakup. Drop size distributions after breakup satisfied Simmons' universal root normal distribution in all three breakup regimes, after removing the core (or drop-forming) drop from the drop population for shear breakup. The size and velocity of the core drop after shear breakup then was correlated successfully based on the observation that the end of drop stripping corresponded to a constant Eötvös number. The relative velocities of the drop liquid were significantly reduced during secondary breakup, due both to large drag coefficients during the drop deformation stage and reduced relaxation times of smaller drops. These effects were correlated successfully based on a simplified phenomenological theory.

Nomenclature

a	=	drop acceleration
C_D	=	drop drag coefficient
$\bar{C}_D$	=	mean drop drag coefficient over breakup periods
d	=	drop diameter
d_{max}, d_{min}	=	maximum and minimum dimensions of a drop
Eo	=	Eötvös number, $a\rho_f d^2/\sigma$ or $g\|\rho_f - \rho_g\|d^2/\sigma$
g	=	acceleration of gravity
MMD	=	mass median diameter
Oh	=	initial Ohnesorge number, $\mu_f/(\rho_f d_o \sigma)^{1/2}$
Oh_{cr}	=	Ohnesorge number of core drop, $\mu_f/(\rho_f d_b \sigma)^{1/2}$
Re	=	Reynolds number, $\rho_g\, d\, u/\mu_g$
SMD	=	Sauter mean diameter
t	=	time
t_b	=	drop breakup time
t*	=	characteristic breakup time, $d_o (\rho_f/\rho_g)^{1/2}/u_o$
u	=	streamwise relative velocity
u'	=	streamwise absolute velocity
We	=	initial Weber number of drop, $\rho_g\, d_o\, u_o^2/\sigma$
We_{cr}	=	Weber number of core drop, $\rho_g\, d_b\, (u_o - u_b)^2/\sigma$
μ	=	molecular viscosity
ρ	=	density
σ	=	surface tension
Subscripts		
b	=	property at end of shear breakup
cr	=	critical conditions for end of shear breakup or onset of breakup
f	=	liquid-phase property
g	=	gas-phase property
o	=	initial condition

Introduction

Numerous studies of secondary drop breakup have been reported due to applications for liquid atomization, industrial and agricultural sprays, dispersed multiphase flows and rainfall, among others. In particular, recent studies suggest that secondary breakup is a rate-controlling process in the near-injector region of pressure-atomized sprays through its affect on drop sizes[1]. Furthermore, primary breakup at the surface of both nonturbulent and turbulent liquids yields drops that intrinsically are unstable to secondary breakup.[2-4] Prompted by these observations, the objective of the present investigation was to extend recent work on secondary breakup caused by well-defined step changes of relative velocities (shock-wave disturbances) in this laboratory.[5]

The following discussion of past research on secondary breakup is brief, see Hsiang and Faeth,[5] Wierzba and Takayama,[6] Giffen and Muraszew,[7] Hinze,[8] Krzeczkowski,[9] and references cited therein for more complete reviews. High-speed photography has been used to identify secondary breakup regimes for shock-wave disturbances.[8-15] Bag breakup is observed at the onset of secondary breakup. This process involves deflection of the center of the drop into a thin bag followed by breakup of both the bag and the liquid ring at its base into drops. Shear breakup is observed at higher relative velocities. This process involves stripping of drops from the periphery of the original drop. Finally, the transition between the bag and shear breakup regimes involves a complex combination of behavior at these two limits. This regime will be termed multimode breakup following Hsiang and Faeth,[5] but also has been called parachute breakup, chaotic breakup, bag-jet breakup and transition breakup.[9,16] Measurements of transitions between breakup regimes have been limited to $\rho_f/\rho_g > 500$ and $Re > 100$.[5,8,9] For these conditions, Hinze[8] shows that breakup regime transitions largely are functions of the ratio of drag to surface tension forces, represented by the Weber number, We, and the ratio of liquid viscous to surface tension forces, represented by the Ohnesorge number, Oh. Hinze[8] found that progressively larger We were required for the onset of breakup as Oh increases because viscous forces

* Graduate Student Research Assistant
† Professor, Fellow AIAA

inhibit drop deformation which is the first step in the breakup process. This behavior has been confirmed by later investigations.[5,9]

The time required for breakup is another aspect of secondary breakup that has received significant attention for shock-wave disturbances at $\rho_f/\rho_g > 500$. For low Oh, it has been found that breakup times normalized by the characteristic breakup time of Ranger and Nicholls,[12] $t^* = d_o(\rho_f/\rho_g)^{1/2}/u_o$, are remarkably independent of the breakup regime and We.[17] As might be expected from the effect of Oh on breakup regimes, however, recent work shows that normalized breakup times tend to increase with increasing Oh.[5] Processes of drop deformation and the variation of the drop drag coefficient with time also appear to scale systematically in terms of t^*.[5]

In comparison to other breakup properties, available information about the outcome of secondary breakup is rather limited. Nevertheless, measurements of drop size distributions for shock-wave disturbances at $\rho_f/\rho_g > 500$ have been reported by Gel'fand et al.[11] and Hsiang and Faeth.[5] Gel'fand et al.[15] observed a bimodal drop size distribution for bag breakup, and suggested that the small drops largely resulted from breakup of the bag and the large drops from breakup of the liquid ring at the base of the bag. However, later measurements of Hsiang and Faeth[5] did not confirm this finding. Instead, drop size distributions satisfied the universal root normal distribution with MMD/SMD = 1.2, proposed by Simmons,[18] which also has been effective for drops within dense sprays and after primary breakup.[1-4] An exception to this behavior was shear breakup, where the distribution was somewhat distorted at large drop sizes. The universal root normal distribution only involves two parameters; therefore, after fixing MMD/SMD, drop sizes are fully specified by the SMD alone. It was found that the SMD for all breakup regimes could be correlated successfully based on a phenomenological analysis of shear breakup.[5] These results, however, raised questions about the mechanism causing secondary breakup to end. In particular, at high values of We, large drops in the size distribution after secondary breakup did not undergo subsequent breakup, even though they were unstable to secondary breakup based on existing breakup criteria — barring unusually large reductions of their relative velocities during the secondary breakup process. Unfortunately, information about drop velocities after secondary breakup was not available, so that the mechanism causing breakup to end could not be resolved. In additions, information about drop size and velocity correlations after secondary breakup clearly is needed for rational estimates of secondary breakup properties in dispersed flows.

The objective of the present investigation was to extend the work of Hsiang and Faeth,[5] in order to resolve the problems of drop size distributions after shear breakup, the mechanism causing breakup to end, and drop size and velocity correlations after secondary breakup. Experimental methods involved shock-wave induced disturbances in air with shadowgraph motion picture photography and pulsed holography used to observe the breakup process. The study was limited to conditions representative of bag, multimode and shear breakup near atmospheric pressure: $\rho_f/\rho_g > 500$, $Oh < 0.039$ and $Re > 100$. Water, n-heptane, ethyl-alcohol and various glycerol mixtures were used as test liquids in order to resolve effects of liquid properties. Phenomenological descriptions of various aspects of secondary breakup were used to help interpret and correlate the measurements.

The paper begins with a discussion of experimental methods. Results are then considered, treating drop size distributions, the properties of the core (or drop-forming) drop when shear breakup ends, and drop velocities after secondary breakup in all three breakup regimes, in turn.

Experimental Methods

Apparatus

The test apparatus was the same as Hsiang and Faeth[5] and only will be described briefly. A shock tube with the driven section open to the atmosphere, similar to Ranger and Nicholls,[12] was used for the experiments. The driven section had a rectangular crossection (38 mm wide × 64 mm high) and a length of 6.7 m with the test location 4.0 m from the downstream end. This provided test times of 17-21 ms in the uniform flow region behind the incident shock wave.

The test location had quartz windows (25 mm high × 305 mm long, mounted flush with the interior the side walls) to allow observation of drop breakup. A drop generator using a vibrating capillary tube, similar to Dabora,[19] was used to generate a stream of drops. This drop stream passed through 6 mm diameter holes in the top and bottom of the driven section, crossing the central plane of the driven section at the test location. An electrostatic drop selection system, similar to Sangiovanni and Kestin,[20] was used to deflect a fraction of the drops out of the stream. This yielded a drop spacing of roughly 7 mm so that drops always were present in the region observed while interactions between drops during secondary breakup were eliminated.

Instrumentation

Drops were observed using pulsed shadowgraph motion pictures and double-pulsed holography. Pulsed shadowgraph motion pictures were used to observe the overall dynamics of breakup, e.g., drop velocities prior to the onset of breakup and the properties of the core drop when the secondary breakup process ended, using an arrangement similar to Hsiang and Faeth.[5] This involved a copper vapor laser as the light source with a 35 mm drum camera used to record shadowgraph images at unity magnification. A function generator was used to pulse the laser when the shock wave neared the drop stream location, with pulse frequencies of 6-8 kHz for 20 pulses. Each laser pulse duration was 30 ns which was sufficient to stop the motion of the drop on the rotating film drum. The drum camera recorded the images with an open shutter within a darkened room. The time between shadowgraph pictures was monitored by recording the signal generator output using a digital oscilloscope. The film records were analyzed using a Gould FD 5000 Image Display. The procedure was to obtain three motion picture shadowgraphs for a particular test condition and group the data to obtain statistically-significant results as ensemble averages. Experimental uncertainties (95% confidence) of the measurements reported here are as follows: initial drop diameter and diameter of the core drop at the end of shear breakup, less than 10%; and velocity of the core drop at the end of shear breakup, less than 15%. Measurements of related breakup properties using this technique — time to the onset of breakup, breakup time and drag coefficients, etc. — are discussed by Hsiang and Faeth.[5]

Double-pulsed holography was used to measure drop size and velocity correlations after secondary breakup. The holocamera and reconstruction systems were similar to earlier work in this laboratory.[1-5] An off-axis arrangement

was used with optics providing a 2-3:1 magnification of the hologram image, with laser pulse times of 20 ns which was sufficient to stop the motion of the drops on film. This was coupled with reconstruction optics that allowed drop diameters as small a 25 μm to be measured with 5% accuracy and drops as small as 10-15 μm to be observed. Reconstruction of the double-pulse holograms yielded two images of the spray with separation times as short as 1 μs. The second pulse was somewhat weaker than the first pulse which allowed directional ambiguity to be resolved because the stronger pulse yielded a sharper reconstructed image. The properties of the reconstructed images were observed using the Gould FD5000 Image Display with a field of view of 1.7 × 2.0 mm. Various locations in the hologram reconstruction were observed by traversing the hologram in two directions and the video camera of the image display in the third direction.

Drops were sized in the same manner as Hsiang and Faeth.[5] The diameters of mildly irregular objects were found by measuring their maximum and minimum diameters through the centroid of the image. Then assuming that the drop had an ellipsoidal shape, the drop diameter was taken to be the diameter of a sphere having the same volume, $d^3 = d_{min}^2 d_{max}$, as the ellipsoid. More irregular images were sized by finding the crossectional area and perimeter of the image and proceeding as before for an ellipsoid having the same properties. The velocity of the drops was found by measuring the distance between the centroid of its two images and dividing by the known time between laser pulses. Results at each condition were summed over at least three realizations, considering 150-300 liquid elements, in order to provide drop size and velocity correlations. Experimental uncertainties caused by the definition of drop diameters are difficult to quantify, however, they are felt to be small in comparison to the accuracy of the size and distance measurements, sampling limitations, and effects of grouping of data when velocities were found for a particular drop size. Estimated experimental uncertainties (95% confidence) based on the latter effects are less than 10% for drop diameters and less than 15% for drop velocities.

Test Conditions

The test conditions are summarized in Table 1. Test drops of water, n-heptane, ethyl alcohol and various glycerol mixtures were used to provide a wide range of liquid properties. The liquid properties listed in Table 1 were obtained from Lange,[21] except for the surface tension of the glycerol mixtures which was measured in the same manner as Wu et al.[2] Initial drop diameters were 1000 μm with the following ranges of other variables: ρ_f/ρ_g = 580-985, Oh = 0.0025-0.39, We = 15-600 and Re = 1060-15080. The We range includes the bag, multimode and shear breakup regimes, which begin at We = 13,35 and 80, respectively, based on the measurements of Hsiang and Faeth.[5] The Re range of the present experiments is higher than conditions where gas viscosity plays a significant role on drop drag properties, e.g. C_D for spheres only varies in the range 0.4-0.5.[22] Shock Mach numbers were relatively low, 1.08-1.31, so that physical properties within the uniform flow region were not significantly different from room air.

Results and Discussion

Drop Size Distributions

It was necessary to address drop size distributions after secondary breakup first because this affects the information needed to characterize secondary breakup properties and drop size and velocity correlations. The main issue to be examined was the distortion of the universal root normal size distribution at large drop sizes after shear breakup, observed by Hsiang and Faeth.[5]

The difficulty with the size distribution function for shear breakup appeared to be due to the presence of the core (or drop forming) drop, which is the remaining portion of the original drop after stripping of smaller drops from its periphery had ended. In particular, the core drop is one of the largest drops in the distribution which corresponded to the region where the measured drop size distribution departed from the universal root normal distribution. Thus, it seemed plausible that the size distribution would approximate the root normal distribution if the core drop was removed from the drop population. A supporting factor was that drop formation by stripping from the surfaces of nonturbulent liquids yields drop size distributions that can be fitted reasonably well by the root normal distribution,[2] while stripping of drops from drops by secondary breakup, and from liquid surfaces by primary breakup, are somewhat similar and yield related correlations for drop sizes.[5]

The resulting drop size distributions after shear breakup, with the core drop removed from the drop population, are illustrated in Fig. 1. These measurements were obtained directly from the data of Hsiang and Faeth.[5] The results are plotted in terms of the root normal distribution function, with the function itself illustrated for values of MMD/SMD = 1.10, 1.20 and 1.50. The measurements are somewhat scattered at large drop sizes because the number of large drops is limited from the breakup of single drops. In view of this effect, the measured drop size distributions are represented reasonably well by the root normal distribution function with MMD/SMD = 1.2. This behavior is similar to drop size distributions after primary breakup and within dense sprays,[1-4] as well as for secondary breakup in the bag and multimode breakup regimes.[5] Thus, the complication of distortion of the drop size distribution for shear breakup can be handled by treating the core drop separately from the population of the drops stripped from the original drop.

As noted earlier, the universal root normal drop size distribution is specified completely if the SMD is known because the only other parameter in the distribution is fixed, e.g., MMD/SMD = 1.2. In principle, the SMD can be found from the correlation given by Hsiang and Faeth[5] which was obtained using results in the bag, multimode and shear breakup regimes. Fortunately, removing the core drop from the drop population when finding the SMD for shear breakup has a negligible effect on this correlation for available test conditions, in comparison to experimental uncertainties. Thus, use of the correlation of Ref. 5 for all three breakup regimes is recommended as before, with the properties of the core drop after shear breakup then added to the distribution. The necessary properties of the core drop will be considered next.

Core Drop Velocity

The velocity and size of the core drop at the end of breakup must be known, in order to treat it separately from

the rest of the drop population after shear breakup. Since drops stripped from the core drop were not observed to undergo subsequent breakup, the end of shear breakup will be taken to coincide with the end of drop stripping from the core drop. In the following, the velocity of the core drop at the end of breakup will be considered first. Then given information about core drop velocities, subsequent stability considerations yield its size.

In order to assist data correlation, a simplified analysis was used to estimate core drop velocities at the end of breakup. The major assumptions of the analysis are as follows: virtual mass, Bassett history and gravitational forces were ignored; gas velocities were assumed to be constant; mass stripping from the core drop was ignored; and a constant average drag coefficient was used over the period of breakup. For present conditions, virtual mass and Basset history forces are small due to the large liquid/gas density ratio of the flow.[23] Similarly, gravitational forces are not a factor because drop motion was nearly horizontal because drag forces were much larger than gravitational forces. Uniform gas velocities, and other gas properties, were a condition of the present experiments. However, the constant core drop mass assumption, taken to be the original drop mass, is questionable. For example, core drop diameters only were 12-30% of the original drop diameter for present test conditions so that the bulk of the original drop mass was lost during stripping. Nevertheless, selecting some other average drop size over the period of breakup only introduces factors on the order of unity so that the original size of the drop was chosen for convenience. Similarly, drop drag coefficients based on the original drop size vary considerably over the drop breakup period. For example, in the deformation period prior to breakup, C_D varies from values of 0.4-0.5 at the start of breakup to 4.8-6.4 when the maximum deformation conditions is reached, over the present test range.[5] Subsequently, values of C_D based on d_o become even larger due to the increased responsiveness of the core drop as it becomes smaller. Nevertheless, the scaling of C_D was such that an effective average value could be found to correlate core drop velocities in spite of the crudeness of the approximations of the analysis.

Based on the previous assumptions, conservation of momentum yields the following equation for the motion of the core drop:

$$du/dt = -3\bar{C}_D \rho_g u^2 / (4 \rho_f d_o) \qquad (1)$$

where the initial relative velocity is equal to u_o and $\bar{C}_D$ is an approximate average over the time of breakup. Integrating Eq. (1) yields the relative velocity of the core drop during the breakup period, as follows:

$$u = u_o / (1 + (3\bar{C}_D\, t/4t^*)(\rho_f/\rho_g)^{1/2}) \qquad (2)$$

Then substituting the breakup time, t_b, into Eq. (2), and rearranging, yields the following expression for the absolute velocity of the core drop at the end of breakup, $u_b' = u_o - u_b$, as follows:

$$(u_b'/u_o)(\rho_f/\rho_g)^{1/2}(1 + 3\bar{C}_D\,(\rho_f/\rho_g)^{1/2}(t_b/t^*)/4)$$

$$= 3\bar{C}_D\,(t_b/t^*)/4 \qquad (3)$$

Earlier work has shown that $t_b/t^* = 5.0$ for $10 < We < 10^6$ and $Oh < 0.1$.[5,17] Thus, the right-hand side of Eq. (3) should be a constant if a constant average value of C_D for the shear breakup process can be found. A reasonable correlation of the present measurements of u_o/u_o was obtained by taking $t_b/t^* = 5.5$, which improved the fit of t_b/t^* for the present test range ($10 < We < 1000$), and $\bar{C}_D = 4.0$, which is comparable to values observed near the maximum deformation condition.[5] This yields $3\,\bar{C}_D\,(t_b/t^*)/4 = 16.5$ on the right-hand side of Eq. (3).

The measurements of core drop velocities at the end of breakup, normalized as suggested by Eq. (3), are plotted as a function of We in Fig. 2. Measurements are shown for all the drop liquids over the test range in the shear breakup regime, $100 < We < 600$, along with the fitted prediction of Eq. (3). The correlation for u_b/u_o is relatively independent of We over this range as anticipated from Eq. (3). The measurements also are in fair agreement with Eq. (3), based on the estimates of t_b/t^* and $\bar{C}_D$ discussed earlier.

The velocity measurements indicated that the relative velocity of the core drop at the end of breakup only was 30-40% lower than the initial relative velocity. This implied that the local Weber numbers of the core drop when breakup ended generally were greater than the critical Weber number for the onset of drop breakup due to shock wave disturbances ($We = 13$). Thus, the criterion for the end of stripping from the core drop differs from the criterion for the onset of breakup. A discussion of this behavior, which leads to an estimation of the core drop diameter, will be considered next.

Core Drop Size

The dynamic state of a drop at the start of secondary breakup, where the drop is round and the drop liquid is motionless, clearly is quite different from the state of the core drop when shear breakup ends, where the drop is deformed and liquid motion associated with drop stripping is present. Thus, it is not surprising that local Weber numbers of the core drop at the end of shear breakup, We_{cr}, are different from (and generally exceed) the critical Weber number associated with the onset of secondary breakup (which implies breakup in the bag breakup regime). Instead, conditions defining the end of stop stripping for shear breakup appear to be related more closely to the onset of breakup for more gradual drop motion, like the breakup of a freely-falling drop. This correspondence is exploited in the following to find a criterion for the end of core drop stripping and a method for estimating the size of the core drop at this condition.

The deformation and size of freely falling drops generally are correlated in terms of Eötvös number. The appropriate expression when drop acceleration is due to gas motion relative to the drop is as follows:[24]

$$Eo = a|\rho_f - \rho_g|\, d^2/\sigma \approx a\, \rho_f d^2/\sigma \qquad (4)$$

where the latter approximation follows because $\rho_f/\rho_g >> 1$ for present test conditions. It is anticipated that drop stripping ends when a critical value of Eötvös number, Eo_{cr}, is reached, based on the behavior of freely-falling drops. The acceleration of the core drop can be found by differentiating Eq. (2) with respect to time, because this expression provided reasonably good estimates of core drop velocities at the end of breakup (cf. Fig. 2). This yields:

$$a = (3\,\bar{C}_D\, u_o/4t^*)(\rho_g/\rho_f)^{1/2} /$$

$$(1 + 3\,\bar{C}_D\, t/4t^*)(\rho_g/\rho_f)^{1/2})^2 \qquad (5)$$

Then evaluating Eq. (5) at $t = t_b$, substituting this value of the acceleration into Eq. (4), and noting that $d = d_b$ at t_b, yields the following expression for the critical Eötvös number at the end of shear breakup:

$$Eo_{cr} = (3\,\bar{C}_D\,We/4)(d_b/d_o)^2\,/$$

$$(1 + (3\,\bar{C}_D\,t_b/4t^*)(\rho_g/\rho_f)^{1/2})^2 \qquad (6)$$

The values of Eo_{cr} were found for all shear breakup conditions, using $t_b/t^* = 5.5$ and $\bar{C}_D = 4.0$ as before. The resulting values of Eo_{cr} for ethyl alcohol, n-heptane and water drops, are plotted as a function of We in Fig. 3. Results for the glycerol mixtures are not included in the plot because an effect of Oh_{cr} was observed, tending to increase Eo_{cr}, that is currently being studied for a wider variation of liquid viscosities. Similar to u_b/u_o in Fig. 2, the critical Eötvös number of the core drop at the end of shear breakup is relatively independent of We and liquid type over the range of the measurements, yielding a mean value, $Eo_{cr} = 16$. This behavior also is similar to the breakup requirements for freely-falling drops, as discussed later.

Given Eo_{cr} and the initial conditions of breakup, Eq. (6) can be solved to find the diameter of the core drop at the end of shear breakup, d_b. It also is of interest to examine the Weber number of the core drop at this condition, We_{cr}. This can be done by finding u_b and d_b from Eqs. (3) and (6) and substituting into the normal definition of the Weber number noting that the relative velocity of the core drop is u_o-u_b, to yield:

$$We_{cr} = 4\,Eo_{cr}\,We/3\,\bar{C}_D)^{1/2}$$

$$(1 + (3\,\bar{C}_D\,t_b/4t^*)(\rho_g/\rho_f)^{1/2}) \qquad (7)$$

Adopting $Eo_{cr} = 16$ and $\bar{C}_D = 4$ as discussed earlier, the coefficient in Eq. (7), $(4\,Eo_{cr}/3\bar{C}_D)^{1/2} = 2.3$, while $t_b/t^* = 5.5$ for the present We range ($10 < 1000$).

Present measurements of We_{cr} for shear breakup are plotted as suggested by Eq. (7) in Fig. 4. Similar to Fig. 3, these results are limited to ethyl alcohol, n-heptane and water drops, pending resolution of the large Oh_{cr} effects observed for the glycerol mixtures. The range of the measurements is $100 < We < 1000$. Finally, Eq. (7) is illustrated on the plot, using the fitted values of Eo_{cr}, $\bar{C}_D$ and t_b/t^* discussed earlier. The scatter of the data is relatively large because products of the measurements are involved, e.g., $We_{cr} = \rho_g d_b(u_o-u_b)^2/\sigma$. Nevertheless, Eq. (7) provides a reasonable fit of the measurements. The results show that the end of drop stripping from the core drop involves a range of We, generally with $We_{cr} > 13$, which is the critical condition for the onset of secondary breakup from shock-wave disturbances. This comes about in the formulation because $We_{cr} \sim We^{1/2}$ in Eq. (7) so that We_{cr} reaches large values as We increases in the shear breakup regime. Nevertheless, drop stripping still ends for the core drop at these high values of We_{cr} because the rate of acceleration of the drop is below critical levels for the gradual variation of drop disturbance levels near the end of the shear breakup process.

It is of interest to compare present values of Eo_{cr} for the end of drop stripping from the core drop during shear breakup with values observed for breakup of freely-falling drops, which also represents a gradual variation of drop disturbance levels. Thus, Table 2 is a summary of Eo_{cr} for the core drop at the end of shear breakup, as well as values of Eo_{cr} measured for freely-falling drops of various liquids in both gases and liquids from Merrington and Richardson,[25] Finlay,[26] Ryan,[27] and Hu and Kintner.[28] The conventional definition of Eötvös number for freely-falling drops is as follows:[24]

$$Eo_{cr} = g\,|\rho_f-\rho_g|\,d^2/\sigma \qquad (8)$$

where d is the maximum stable drop diameter and ρ_g should be interpreted as the density of the continuous phase, and is a liquid in the case of freely-falling drops in liquids. In addition to Eo_{cr}, the table provides the values of d, ρ_f, μ_f, σ, Oh_{cr} and We_{cr} for the various breakup processes.

For conditions at the end of shear breakup in Table 2, d_b, Oh_{cr} and We_{cr} vary over ranges set by present test conditions, which is evident from Fig. 4, even though Eo_{cr} is relatively constant. In contrast, stable freely-falling drop conditions involve single values of d, Oh_{cr} and We_{cr} for given drop and continuous phases. In this case, We_{cr} and Eo_{cr} are closely related because the freely-falling drops eventually stabilize at their terminal velocity where the maximum value of We is reached. Remarkably, the average values of Eo_{cr} are not very different for the end of shear breakup and for the onset of breakup for freely-falling drops in both gases and liquids, 16 and 12, respectively. Differences of this order certainly are reasonable because one process involves the end of drop stripping from the core drop, while the other represents a limit for the onset of bag breakup.[24]

Loparev[28] reports We_{cr} for the onset of drop breakup, generally by bag breakup, curing gradually accelerating and decelerating gas flows in converging and diverging passages having various rates of crossectional area change with distance. An extensive range of test conditions was studied but unfortunately the information provided is not sufficient to find values of Eo_{cr}. Nevertheless, values of We_{cr} for low-Oh_{cr} drops are similar to those in Table 2 for freely-falling drops, suggesting similar values of Eo_{cr} as well. An interesting aspect of these measurements is that We_{cr} increases with increasing Oh_{cr} for glycerol mixtures, similar to behavior observed during the present study for the end of shear breakup. This is not surprising due to past observations of increasing We at the onset of breakup for shock-wave disturbances as Oh increases.[5,8,9] Pending resolution of this issue, however, the present value of Eo_{cr} should be used with caution to find core drop properties when values of Oh_{cr} are larger than the present test range, e.g., when $Oh_{cr} > 0.032$.

The previous considerations suggest that We, Eo and time all are factors in drop breakup events at low Oh. These interactions are highlighted by the local values of We_{cr}, Eo_{cr} and t_{cr}/t^* for various breakup events summarized in Table 3. For abrupt disturbances, like the onset of secondary breakup for shock-wave disturbances, local values of We_{cr} and Eo_{cr} were estimated at the time of breakup using measured values of drop drag in the deformation period; these values are lower than criteria normally given for breakup regime transitions due to drop acceleration prior to the onset of breakup.[5] Similar to the normalized breakup time, the normalized time at the onset of breakup for shock-wave disturbances is constant over a wide range of We, $t_{cr}/t^* = 1.6$. For this process, drops in the deformation period have local values of We and Eo that exceed limits for the onset of breakup, however, breakup does not begin until the drop has had time to deform and achieve a dynamical condition in the liquid that allows drops to divide or separate from the parent drop. The characteristics of We_{cr}, Eo_{cr} and t_{cr}/t^* are somewhat different for gradual disturbances. In the case of bag breakup

for a freely-falling drop, Eo is a maximum at the start of free fall while t_{cr}/t^* is large due to the relatively slow acceleration of the drop. Thus, liquid properties are roughly quasisteady at each relative velocity condition and breakup only occurs when forces on the drop surface due to drag are too large to be stabilized by surface tension, i.e., when the Weber number of the drop reaches a critical value. Finally, the end of drop stripping for shear breakup also involves near quasisteady liquid behavior with the dynamical state of the drop being stabilized by surface tension once the forces on the surface, represented by the drop acceleration, became lower than a critical value represented by Eo_{cr}. A range of We_{cr} is associated with this condition due to the large variation of the drag coefficient with the degree of deformation of the drop. Thus, various breakup events are associated with required minimum values of We, Eo and time, with one of these parameters frequently serving as the controlling parameter for a particular process.

Drop-Size/Velocity Correlation

The last aspect of secondary breakup considered was the drop-size/velocity correlation at the completion of secondary breakup. These results will include all the drops in the bag and multimode breakup regimes. However, the core drop will be excluded in the shear breakup regime because its properties have already been established.

A simplified analysis, along the lines of the analysis for core drop velocities, was used to assist correlation of the drop velocity data. This involves neglecting virtual mass, Bassett history and gravitational forces, taking gas properties to be constant, and assuming that a constant average drag coefficient was appropriate for all drop sizes over the period of breakup, as before. Additionally, the time in the breakup process when a particular drop was formed was not considered. Instead, drop motion for a particular drop size was found assuming that the drop was present as a separate drop throughout the breakup process. This clearly is a crude approach but it did yield a simple algebraic formula that was effective for interpreting and correlating the velocity measurements.

Based on these assumptions, the governing equation of conservation of momentum for a particular drop size of diameter d is as follows:

$$du/dt = -3\bar{C}_D\rho_g u^2 / (4 \rho_f d) \qquad (9)$$

Integrating Eq. (9) from t=0, where $u = u_o$ to $t = t_b$ where $u = u_b$, then yields:

$$u_o/u_b = 1 + 3\bar{C}_D(t_b/t^*)(\rho_g/\rho_f)^{1/2}(d_o/d) \qquad (10)$$

Present measurements of drop velocities after secondary breakup are plotted as suggested by Eq. (10) in Fig. 5. These test results involve all the drop liquids over the data range summarized in Table 1. This includes bag, multimode and shear breakup but with the results for the core drop excluded for shear breakup. A prediction based on Eq. (10) also is shown on the plot. The prediction involves t_b/t^* = 5.5 as before, however, the mean drag coefficient was changed from the value used for the core drop to $\bar{C}_D = 1.1$, in order to improve the fit of predictions and measurements for large drops

The results illustrated in Fig. 5 show that the relative velocities are reduced by 30-70% over the period of breakup with the smallest drops experiencing the largest reduction, as anticipated. The best fit prediction of Eq. (10) is only in fair agreement with the measurements: the relative velocities of larger drops are overestimated while the relative velocities of smaller drops are substantially underestimated. These deficiencies follow from the approximations of the simplified theory. In particular, a single average drag coefficient is not appropriate for all drop sizes, with the larger drops having larger drag coefficients than $\bar{C}_D = 1.1$ due to their deformation,[5] which accounts for overestimating their relative velocities. Additionally, the smaller drops form late in the breakup process so that their faster response only is effective for a fraction of t_b, which accounts for underestimating their velocities. Nevertheless, drop velocities after secondary breakup correlate reasonably well in terms of the variables used in Fig. 5, and the empirical correlation shown on the figure provides a reasonably good drop-size/velocity correlation.

Conclusions

The outcome of secondary breakup after shock wave initiated disturbances was studied, considering drops of water, n-heptane, ethyl-alcohol and glycerol in air at normal temperature and pressure (We of 15-600, Oh of 0.0025-0.039, ρ_f/ρ_g of 579-985 and Re = 1060-15080). The major conclusions of the study are as follows:

1. Earlier problems with the drop size distribution after shear breakup,[5] were resolved by removing the core drop from the drop population and treating it separately. With this change, drop sizes after breakup in all three breakup regimes satisfy Simmons' universal root normal distribution with MMD/SMD = 1.2.

2. The velocity and size of the core drop after shear breakup were correlated successfully based on simplified considerations of drop motion during breakup (Eq. (3)) and the observation that the Eötvös number at the end of drop stripping was a constant (Eq. (6)), i.e., $Eo_{cr} = 16$.

3. The relative velocities of the drop liquid are significantly reduced during secondary breakup (30-70%, depending on drop size) due to both the large drag coefficients during the drop deformation stage and the reduced relaxation times of smaller drops. These effects were correlated successfully based on variables found from simplified analysis of drop motion (Fig. 5).

4. At low Oh, criteria for various drop breakup processes can be represented by critical values of We, Eo and t/t^*. While certain minimum values are required for all three parameters, reaching a critical local value of one of the parameters tends to control the onset of particular breakup events: t_{cr}/t^* for the onset of breakup after a shock-wave disturbance, We_{cr} for the onset of breakup of a freely-falling drop, and Eo_{cr} for the end of drop stripping from the core drop during shear breakup.

Present findings generally were limited to Oh < 0.039, with results concerning core drop properties limited to Oh < 0.011. Increasing Oh tends to impede drop deformation and breakup processes and should modify secondary breakup behavior from results observed during the present study. These effects of Oh merit additional study in order to better understand secondary breakup properties.

Acknowledgments

This research was sponsored by the Air Force Office of Scientific Research, Grant Nos. AFOSR-89-0516 and F49620-92-J-0399, under the technical management of J. N. Tishkoff. The authors would like to thank C. W. Kauffman for loan of shock tube facility and advice concerning its operation. The U.S. Government is authorized to reproduce and distribute copies for governmental purposes notwithstanding any copyright notation thereon.

References

[1]Ruff, G.A., Wu, P.-K., Bernal, L. P. and Faeth, G.M., "Continuous- and Dispersed-Phase Structure of Dense Nonevaporating Pressure-Atomized Sprays," J. Prop. Power, Vol. 8, 1992, pp. 280-289.

[2]Wu, P.-K., Ruff, G.A. and Faeth, G.M., "Primary Breakup in Liquid/Gas Mixing Layers for Turbulent Liquids," Atomization and Sprays, Vol. 1, 1991, pp. 421-440.

[3]Wu, P.-K., Tseng, L.-K. and Faeth, G.M., "Primary Breakup in Gas/Liquid Mixing Layers for Turbulent Liquids," Atomization and Sprays, Vol. 2, 1992, pp. 295-317.

[4]Wu, P.-K. and Faeth, G.M., "Aerodynamic Effects on Primary Breakup of Turbulent Liquids," AIAA Paper No. 93-0903, 1993.

[5]Hsiang, L.-P. and Faeth, G.M., "Near-Limit Drop Deformation and Secondary Breakup," Int. J. Multiphase Flow, Vol. 18, 1992, pp. 635-652.

[6]Wierzba, A. and Takayama, K., "Experimental Investigations on Liquid Droplet Breakup in a Gas Stream," Rep. Inst. High Speed Mech., Tohoku Univ., Vol. 53, No. 382, 1987, pp. 1-99.

[7]Giffen, E. and Muraszew, A., *The Atomization of Liquid Fuels*, Chapman and Hall, London, 1953.

[8]Hinze, J.O., "Fundamentals of the Hydrodynamic Mechanism of Splitting in Dispersion Processes," AIChE J., Vol. 1, No. 3, 1955, pp. 289-295.

[9]Krzeczkowski, S.A., "Measurement of Liquid Droplet Disintegration Mechanisms," Int. J. Multiphase Flow, Vol. 6, 1980, pp. 227-239.

[10]Hanson, A.R., Domich, E.G. and Adams, H.S., "Shock-tube Investigation of the Breakup of Drops by Air Blasts," Phys. Fluids, Vol. 6, No. 8, 1963, pp. 1070-1080.

[11]Gel'fand, B.E, Gubin, S. A. and Kogarko, S. M., "Various Forms of Drop Fractionation in Shock Waves and Their Special Characteristics," Inzhenerno-Fizicheskii Zhurnal, Vol. 27, No. 1, 1974, pp. 119-126.

[12]Ranger, A.A. and Nicholls, J.A., "The Aerodynamic Shattering of Liquid Drops," AIAA J. Vol. 7, 1969, pp. 285-290.

[13]Reinecke, W.G. and McKay, W.L., "Experiments on Waterdrop Breakup Behind Mach 3 to 12 Shocks," Sandia Corp. Rept. SC-CR-70-6063, 1969.

[14]Reinecke, W.G. and Waldman, G.D., "A Study of Drop Breakup Behind Strong Shocks with Applications to Flight," Avco Rept. AVSD-0110-70-77, 1970.

[15]Wierzba, A. and Takayama, K., "Experimental Investigation of the Aerodynamic Breakup of Liquid Drops," AIAA J., Vol. 26, No. 11, 1988, pp. 1329-1335.

[16]Borisov, A.A., Gel'fand, B.E., Natanzon, M.S. and Kossov, O.M., "Droplet Breakup Regimes and Criteria for Their Existence," Inzhenerno-Fizicheskii Zhurnal, Vol. 40, No. 1, 1981, pp. 64-70.

[17]Liang, P.Y., Eastes, T.W. and Gharakhari, A., "Computer Simulations of Drop Deformation and Drop Breakup," AIAA Paper No. 88-3142, 1988.

[18]Simmons, H.C., "The Correlation of Drop-Size Distributions in Fuel Nozzle Sprays," J. Engr. for Power Vol. 99, 1977, pp. 309-319.

[19]Dabora, E.K, "Production of Monodisperse Sprays," Rev. Sci. Inst., Vol. 38, 1967, pp. 502-506.

[20]Sangiovanni, J. and Kestin, A.S., "A Theoretical and Experimental Investigation of the Ignition of Fuel Droplets," Combust. Sci. Tech., Vol. 16, Nos. 1 and 2, 1977, pp. 59-70.

[21]Lange, N.A., *Handbook of Chemistry*, 8th ed., Handbook Publishers, Inc., Sandusky, Ohio, 1952, pp. 1134 and 1709.

[22]White, F.M., *Viscous Fluid Flow*, McGraw-Hill, New York, 1974.

[23]Faeth, G.M., "Mixing, Transport and Combustion in Sprays," Prog. Energy Combust. Sci. Vol. 13, 1987, pp. 293-345.

[24]Clift, R., Grace, J.R. and Weber, M.E., *Bubbles, Drops and Particles*, Academic Press, New York, 1978, pp. 26 and 339-347.

[25]Merrington, A.C. and Richardson, E.G., "The Break-Up of Liquid Jets," *Proc. Phys. Soc. (London)*, Vol. 59, 1947, pp. 1-13.

[26]Finlay, B.A., Ph.D. Thesis, University of Birmingham, 1957.

[27]Ryan, R.T., "The Behavior of Large Low-Surface-Tension Water Drops Falling at Terminal Velocity in Air," J. Appl. Meterology, Vol. 15, 1976, pp. 157-165.

[28]Hu, S. and Kintner, R.C., "The Fall of Single Drops Through Water," AIChE J., Vol. 1, 1955, pp. 42-48.

[29]Loparev, V.P., "Experimental Investigation of the Atomization of Drops of Liquid Under Conditions of a Gradual Rise of the External Forces," Izvestiya Akademii Nauk SSSR, Mekhanika Zhidkosti i Gaza No. 3, 1975, pp. 174-178.

Table 1 Summary of test conditions[a]

Drop Liquid	ρ_f (kg/m^3)	$\mu_f \times 10^4$ (kg/ms)	$\sigma \times 10^3$ (N/m)	Oh (-)	We (-)	Re (-)
water	997	8.94	70.8	0.0038	15-600	1990-15080
n-heptane	683	3.94	20.0	0.0025	15-600	1060-7200
ethyl-alcohol	800	16.0	24.0	0.011	15-600	1150-7880
glycerol (42%)[b]	1105	35.0	65.4	0.012	15-375	1910-10790
glycerol (63%)[b]	1162	108.0	64.8	0.039	15-37	1880-10640

[a]Breakup in air initially at 98.8 kPa and 2.97 ± 2K in driven section of shock tube with shock Mach numbers in the range 1.08-1.31. Properties of air taken at normal temperature and pressure: $\rho_g = 1.18$ kg/m^3, $\mu_g = 18.5 \times 10^{-5}$ kg/ms.
[b]Percent glycerin by mass.

Table 2 Eo_{cr} for gradual termination and initiation of drop breakup

Drop Liquid	d (mm)	ρ_f (kg/m^3)	$\mu_f \times 10^4$ (kg/ms)	$\sigma \times 10^3$ (N/m)	Oh_{cr} (-)	We_{cr} (-)	Eo_{cr} (-)
a. End of shear breakup.							
In air, present study:							
water	0.15-0.30	997	8.9	71	0.007-0.010	15.1-28.5	17.5
n-heptane	0.12-0.26	694	4.0	20	0.007-0.010	7.8-16.0	14.9
ethyl alcohol	0.13-0.29	800	16.0	24	0.021-0.032	10.5-19.0	14.4
b. Initation of bag breakup of freely-falling drops.							
In air, Merrington and Richardson:[25]							
water	10.0	1000	9.8	72	0.0012	---	13.5
carbon tetachloride	3.6	1577	7.8	41	0.0018	---	8.0
In air, Finley:[26]							
water	8.0	1000	9.8	72	0.0013	11.0	8.5
tetrabromomethane	3.5	2950	92.9	36	0.0150	12.0	7.2
In air, Ryan:[27]							
water	9.1	1000	9.8	72	---	12.2	11.2
water+surfactant	7.5	1000	---	50	---	12.4	11.1
water+surfactant	6.9	1000	---	40	---	---	11.6
water+surfactant	6.1	1000	---	33	---	14.5	12.2
water+surfactant	5.2	1000	---	25	---	---	10.6
water+surfactant	4.7	1000	---	20	---	---	10.9
water+surfactant	4.4	1000	---	17	---	12.0	11.0
In water, Hu and Kintner:[28]							
tetabromomethane	5.1	2950	92.9	36	0.0126	7.4	13.8
dibromoethane	6.7	2150	15.8	32	0.0023	8.2	16.0
ethyl bromide	9.1	1448	4.9	30	0.0008	7.0	12.3
nitrobenzene	15.4	1195	17.4	24	0.0026	8.6	19.1
bromobenzene	11.3	1488	10.7	38	0.0013	7.8	13.5
tetrachloroethylene	10.4	1614	9.0	44	0.0010	8.2	14.8
carbon tetrachloride	10.4	1577	7.8	41	0.0009	7.9	15.1

Table 3 Criteria for secondary breakup processes[a]

Process	We_{cr}	Eo_{cr}	t_{cr}/t^*
Abrupt (shock-wave) disturbances:			
Start of bag breakup (in gases)	8-23	24-70	1.6
Start of multimode breakup (in gases)	23-53	70-160	1.6
Start of shear breakup (in gases)	53 <	160 <	1.6
Gradual disturbances:			
Start of bag breakup (in gases)[b]	11-13	11	large
Start of bag breakup (in liquids)[b]	7-9	15	large
End of shear breakup (in gases)	8-29[c]	16	5.5

[a]$Oh < 0.05$, We_{cr} and Eo_{cr} subsequently increase with increasing Oh.
[b]Freely-falling drops in a motionless environment.
[c]Present test range with wider range probable.

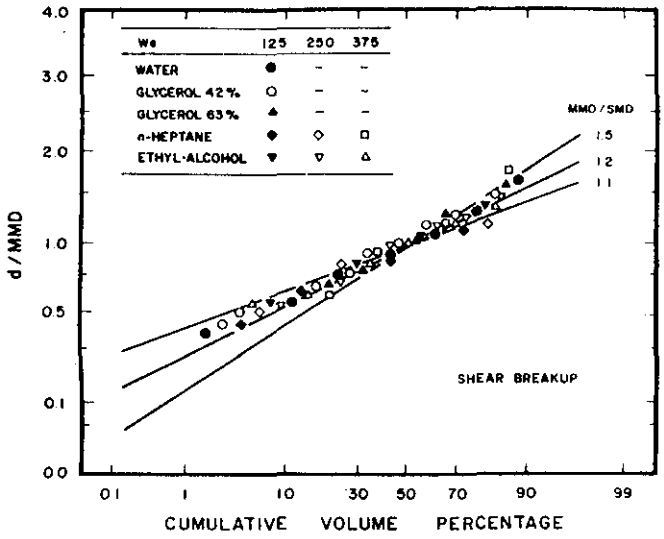

Figure 1 Drop diameter distribution after shear breakup, excluding the core drop.

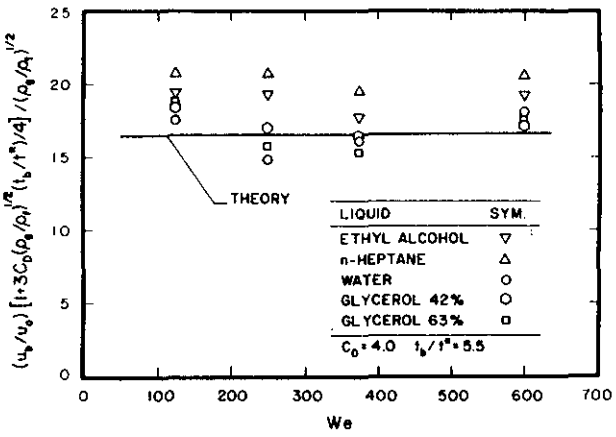

Figure 2 Velocities of the core drop at the end of shear breakup.

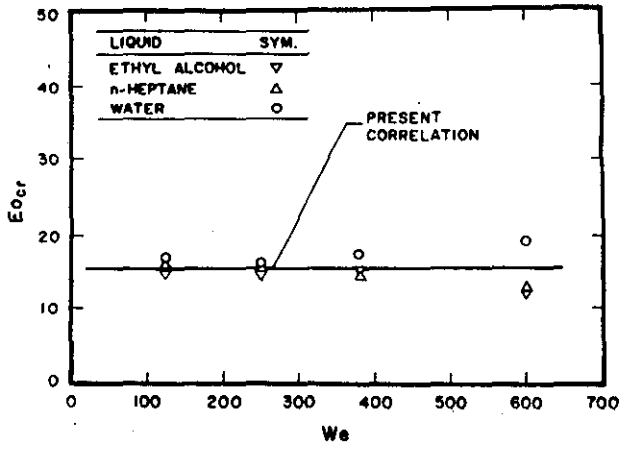

Figure 3 Critical Eötvös number of the core drop at the end of shear breakup.

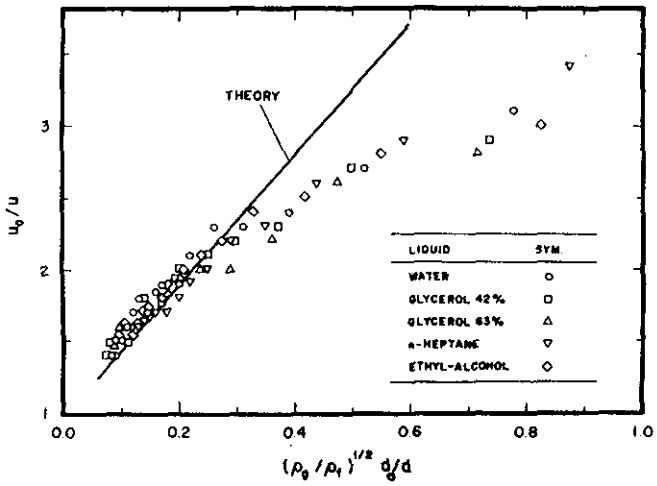

Figure 5 Correlation of drop velocities after secondary breakup as a function of drop size.

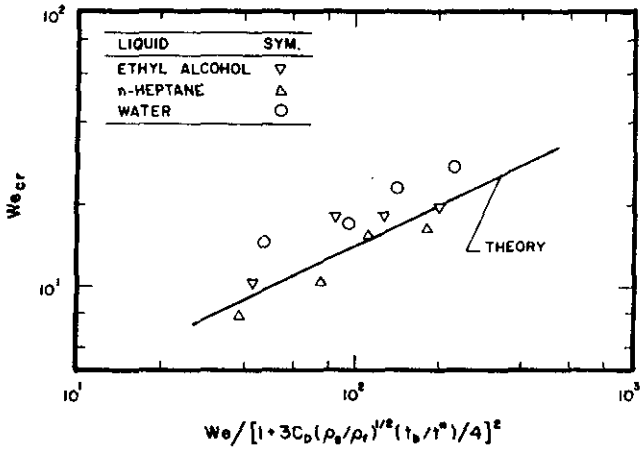

Figure 4 Critical Weber numbers of the core drop at the end of shear breakup.